J|A|C|S ARTICLES

Published on Web 12/11/2008

Impaired Acid Catalysis by Mutation of a Protein Loop Hinge Residue in a YopH Mutant Revealed by Crystal Structures

Tiago A. S. Brandão,[†] Howard Robinson,[‡] Sean J. Johnson,*[,†] and Alvan C. Hengge*[,†]

Department of Chemistry and Biochemistry, Utah State University, Logan, Utah 84322-0300, and Biology Department, Brookhaven National Laboratory, Upton, New York 11973-5000

Received September 23, 2008; E-mail: alvan.hengge@usu.edu; sean.johnson@usu.edu

Abstract: Catalysis by the *Yersinia* protein-tyrosine phosphatase YopH is significantly impaired by the mutation of the conserved Trp354 residue to Phe. Though not a catalytic residue, this Trp is a hinge residue in a conserved flexible loop (the WPD-loop) that must close during catalysis. To learn why this seemingly conservative mutation reduces catalysis by 2 orders of magnitude, we have solved high-resolution crystal structures for the W354F YopH in the absence and in the presence of tungstate and vanadate. Oxyanion binding to the P-loop in W354F is analogous to that observed in the native enzyme. However, the WPD-loop in the presence of oxyanions assumes a half-closed conformation, in contrast to the fully closed state observed in structures of the native enzyme. This observation provides an explanation for the impaired general acid catalysis observed in kinetic experiments with Trp mutants. A 1.4 Å structure of the W354F mutant obtained in the presence of vanadate reveals an unusual divanadate species with a cyclic $[VO]_2$ core, which has precedent in small molecules but has not been previously reported in a protein crystal structure.

Introduction

Protein tyrosine phosphatases (PTPs) comprise a large family of enzymes responsible for the dephosphorylation of intracellular Tyr residues, functioning in concert with protein tyrosine kinases (PTKs) to modulate important signal transduction pathways.[1−5] For example, the breakdown in regulation of tyrosine phosphorylation levels is involved in many human diseases, including cancer and diabetes.[6] The PTPs are also involved in a number of bacterial and viral strategies to disrupt host signal transduction pathways. For example, the PTP YopH is an essential virulence factor in the bacteria *Yersinia* sp. This genus includes three species causative of human illness, ranging from gastrointestinal disease to Bubonic Plague.[7]

YopH is one of the most powerful phosphatases, catalyzing the hydrolysis of phosphate monoester dianions with k_{cat} values[8] of about 1300 s^{-1} with practically no dependence on the basicity of the leaving group ($\beta_{lg} = -0.008$).[9] Relative to the rate constant for the uncatalyzed reaction of $\sim 10^{-20}$ s^{-1}, YopH ranks as one of the most efficient enzymes known in terms of catalytic efficiency.[10]

The binding pocket in PTPs is comprised primarily of the "P-loop", a phosphate binding loop with the consensus sequence $C(X)_5R(S/T)$. This loop contains the nucleophilic cysteine and an arginine that hydrogen-bonds to the phosphoryl group of the substrate and aids in transition-state stabilization.[11,12] The second component of the active site in PTPs is an adjacent flexible loop including a conserved WPD sequence. This region is known as the WPD-loop and includes the catalytically important Asp residue that functions as a general acid in formation of the phosphocysteine intermediate and as a general base in its subsequent hydrolysis.[13,14]

The first evidence for the flexibility of the WPD-loop came from comparisons of X-ray structures of PTPs in the presence and in the absence of bound oxyanions. These structures show that the WPD-loop has two distinct conformations, an "open" conformation in which the WPD-loop has negligible interaction with the P-loop, and a "closed" conformation, where the WPD-loop is folded over the active site, bringing the conserved Asp residue up to 8 Å closer and into hydrogen-bonding distance of the bound oxyanion.[15−19] Figure 1 shows the change in

[†] Utah State University.
[‡] Brookhaven National Laboratory.

(1) Hunter, T. *Cell* **1995**, *80*, 225–236.
(2) Barford, D.; Das, A. K.; Egloff, M.-P. *Annu. Rev. Biophys. Biomol. Struct.* **1998**, *27*, 133–164.
(3) Jackson, M. D.; Denu, J. M. *Chem. Rev.* **2001**, *101*, 2313–2340.
(4) Zhang, Z.-Y. *Crit. Rev. Biochem. Mol. Biol.* **1998**, *33*, 1–52.
(5) Cleland, W. W.; Hengge, A. C. *Chem. Rev.* **2006**, *106*, 3252–3278.
(6) Zhang, Z. Y. *Curr. Opin. Chem. Biol.* **2001**, *5*, 416–23.
(7) Brubaker, R. R. *Clin. Microbiol. Rev.* **1991**, *4*, 309–24.
(8) Zhang, Z. Y.; Clemens, J. C.; Schubert, H. L.; Stuckey, J. A.; Fischer, M. W. F.; Hume, D. M.; Saper, M. A.; Dixon, J. E. *J. Biol. Chem.* **1992**, *267*, 23759–23766.
(9) Keng, Y. F.; Wu, L.; Zhang, Z. Y. *Eur. J. Biochem.* **1999**, *259*, 809–814.
(10) Lad, C.; Williams, N. H.; Wolfenden, R. *Proc. Natl. Acad. Sci. U.S.A.* **2003**, *100*, 5607–5610.
(11) Guan, K. L.; Dixon, J. E. *J. Biol. Chem.* **1991**, *266*, 17026–17030.
(12) Zhang, Z. Y.; Wang, Y.; Wu, L.; Fauman, E. B.; Stuckey, J. A.; Schubert, H. L.; Saper, M. A.; Dixon, J. E. *Biochemistry* **1994**, *33*, 15266–70.
(13) Zhang, Z. Y. *Curr. Top. Cell Regul.* **1997**, *35*, 21–68.
(14) Zhang, Z. Y.; Wang, Y. A.; Dixon, J. E. *Proc. Natl. Acad. Sci. U.S.A.* **1994**, *91*, 1624–1627.
(15) Barford, D.; Flint, A. J.; Tonks, N. K. *Science* **1994**, *263*, 1397–1404.

 10.1021/ja807418b CCC: $40.75

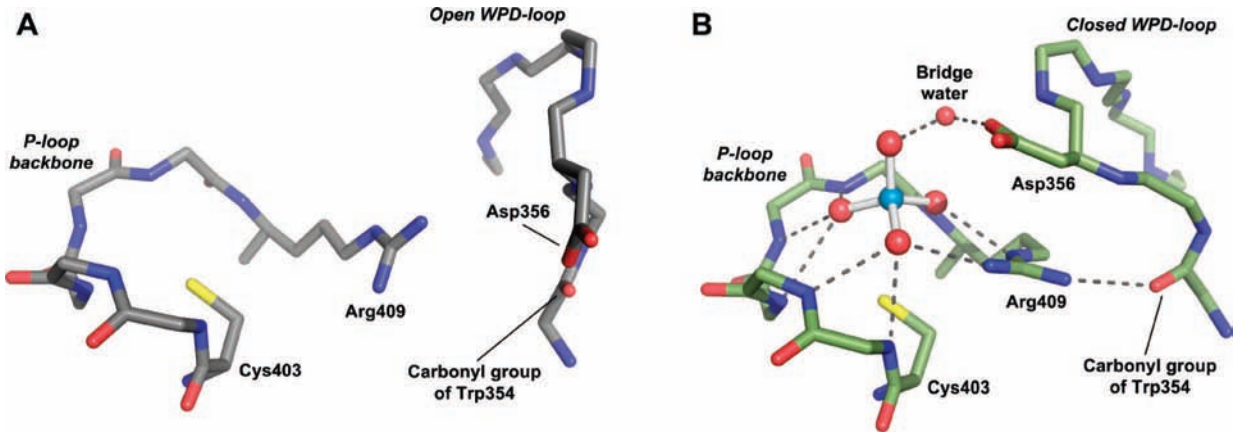

Figure 1. Orientations of selected residues at the active site of YopH in the unbound (A) and tungstate-bound states (B). Hydrogen bonds are present between the oxyanion and the backbone amide groups of the P-loop as well as with Arg409. Upon tungstate binding, this residue rotates to form two hydrogen bonds to the oxyanion, resulting in a new hydrogen bond with the carbonyl oxygen of Trp354. Associated movement of the WPD-loop brings Asp356 into position to function as a general acid during catalysis. The tungstate-bound crystal structure was obtained at a pH where the Asp356 is deprotonated, and therefore, to avoid electrostatic repulsion, a bridge water molecule assumes a position between the oxyanion and the Asp356 carboxylate.[17] The representations were prepared with the program PyMol[20] from the structures 1YPT[16] and 1YTW.[17]

orientations of key residues in the active site of YopH. Upon oxyanion or substrate binding, the conserved Arg residue rotates to make two hydrogen bonds with the oxyanion. A new hydrogen bond is also formed between the guanidinium group of Arg409 and the carbonyl oxygen atom of Trp354. These interactions are associated with movement of the WPD-loop in attaining the closed position.

Complementary to the crystal structures, WPD-loop dynamics of YopH in solution have been studied experimentally and theoretically. Experimental studies include time-resolved fluorescence anisotropy, steady-state fluorescence, ultraviolet resonance Raman (UVRR) spectroscopy,[21] relaxation kinetics,[22] H/D exchange, and electrospray ionization Fourier transform ion cyclotron resonance mass spectrometry.[23] Theoretical examinations consist of molecular dynamics (MD) simulations.[24] These studies all verify that the WPD-loop in apo YopH alternates between the open and partially closed conformations in solution, with estimates of frequency from the nanosecond to the millisecond range. In the solid state, although only two conformations have been observed, significantly higher thermal *B*-factors for the open than the closed conformation also support the idea that the WPD-loop is flexible.[19] Moreover, relaxation kinetic studies show that oxyanion binding pushes the equilibrium toward the closed form (Scheme 1).[22]

General acid catalysis by the conserved Asp residue is a critical aspect of the powerful YopH catalyst. Kinetic isotope effects (KIEs) have shown that proton transfer to the leaving group is complete in the transition state, verifying that WPD-loop isomerization brings the general acid into position, permitting full neutralization of the leaving group. Loss of acid catalysis by mutation of Asp 356 to Asn results in a rate reduction of 3 orders of magnitude.[14] Previous kinetic studies have shown that mutation of the WPD-loop residue Trp354 to phenylalanine significantly impairs general acid catalysis.[9,25] Catalysis is reduced by ~2 orders of magnitude, and KIEs reveal that the leaving group is only partially neutralized in the transition state.[25] These results were proposed to be related to impairment of WPD-loop movement. Previous research has explored the relationships in model systems between distance and positioning between proton donor and acceptor and the efficiency of acid catalysis.[26,27] Such factors are even more important for proton transfer than for nucleophilic attack.[28] Here, we show that the reduced catalysis and impaired proton-transfer efficiency in W354F YopH result from an inability of the WPD-loop to attain a fully closed position, preventing the general acid from assuming the proper position for full proton transfer in the transition state. These findings afford a better understanding of the conformational dynamics involved in WPD-loop closure and provide a snapshot of WPD-loop movement during closure. Our observations also include an unusual divanadate species observed at the active site of the mutant W354F YopH, which has precedent in small molecules but has not been previously reported in a protein structure.

Scheme 1. Substrate Binding Model for YopH with Rate Constants Obtained from Relaxation Kinetics at 35 °C[a]

$$E_{open}^{apo} + L \underset{1.7\ \mu s^{-1}}{\overset{1.7\times10^{9}\ M^{-1}.s^{-1}}{\rightleftharpoons}} E_{open}\cdot L \underset{0.23\ \mu s^{-1}}{\overset{0.016\ \mu s^{-1}}{\rightleftharpoons}} E_{close}\cdot L$$

[a] L is the ligand *p*-nitrocatechol sulfate.[22]

Materials and Methods

Protein Expression and Purification. The plasmid encoding the mutant W354F of *Yersinia* PTP (also referred to in the

(16) Stuckey, J. A.; Schubert, H. L.; Fauman, E. B.; Zhang, Z. Y.; Dixon, J. E.; Saper, M. A. *Nature* **1994**, *370*, 571–575.
(17) Fauman, E. B.; Yuvaniyama, C.; Schubert, H. L.; Stuckey, J. A.; Saper, M. A. *J. Biol. Chem.* **1996**, *271*, 18780–18788.
(18) Groves, M. R.; Yao, Z. J.; Roller, P. P.; Burke, T. R.; Barford, D. *Biochemistry* **1998**, *37*, 17773–17783.
(19) Schubert, H. L.; Fauman, E. B.; Stuckey, J. A.; Dixon, J. E.; Saper, M. A. *Protein Sci.* **1995**, *4*, 1904–1913.
(20) DeLano, W. L. *PyMol*; DeLano Scientific: Palo Alto, CA, 2007.
(21) Juszczak, L. J.; Zhang, Z. Y.; Wu, L.; Gottfried, D. S.; Eads, D. D. *Biochemistry* **1997**, *36*, 2227–2236.
(22) Khajehpour, M.; Wu, L.; Liu, S. J.; Zhadin, N.; Zhang, Z. Y.; Callender, R. *Biochemistry* **2007**, *46*, 4370–4378.
(23) Wang, F.; Li, W. Q.; Emmett, M. R.; Hendrickson, C. L.; Marshall, A. G.; Zhang, Y. L.; Wu, L.; Zhang, Z. Y. *Biochemistry* **1998**, *37*, 15289–15299.
(24) Hu, X.; Stebbins, C. E. *Biophys. J.* **2006**, *91*, 948–956.
(25) Hoff, R. H.; Hengge, A. C.; Wu, L.; Keng, Y. F.; Zhang, Z.-Y. *Biochemistry* **2000**, *39*, 46–54.
(26) Kirby, A. J.; Dutta-Roy, N.; Silva, D.; Goodman, J. M.; Lima, M. F.; Roussev, C. D.; Nome, F. *J. Am. Chem. Soc.* **2005**, *127*, 7033–7040.
(27) Orth, E. S.; Brandao, T. A. S.; Milagre, H. M. S.; Eberlin, M. N.; Nome, F. *J. Am. Chem. Soc.* **2008**, *130*, 2436–2437.
(28) Kirby, A. J. *Acc. Chem. Res.* **1997**, *30*, 290–296.

literature as YopH or Yop51*Δ162) was provided by Dr. Z.-Y. Zhang (Department of Biochemistry and Molecular Biology, Indiana University School of Medicine) and has been previously reported.[9] Expression in *Escherichia coli* BL21(DE3) was under the control of the T7 promoter. Purification was accomplished by a slight modification of the previously described method.[9] Briefly, *E. coli* BL21(DE3) W354F cells from an overnight culture (10 mL) were diluted to 1 L of 2xYT containing 100 μg/mL ampicillin. The cells were grown at 37 °C to an optical density of 0.8 at 600 nm, induced with isopropyl β-D-thiogalactoside (IPTG) to a final concentration of 0.4 mM, and grown for an additional 20 h at room temperature. The cells were then harvested by centrifugation at 8000 rpm for 30 min. The next steps were carried out at 4 °C. The resulting pellet (10 g) was resuspended in 40 mL of buffer A (100 mM sodium acetate, 100 mM NaCl, 1 mM EDTA, and 1 mM DTT, pH 5.7) containing protease inhibitors (2 mM benzamidine and 200 μg/mL each of aprotinin, pepstatin, and leupeptin). The cells were lysed by sonication and spun down at 20 000 rpm for 30 min. The supernatant was filtered through a 0.45 μM PES filter to remove residual debris and loaded on a 5 mL HiTrap SP HP column at 1.5 mL/min. The column was washed with buffer A until the absorbance at 280 nm was zero. The protein was eluted at 2 mL/min with a 150 mL linear gradient from 0.1 to 0.5 M NaCl in buffer A. The fractions with protein were pooled, concentrated to 5 mL, and eluted with buffer A on a 320 mL HiLoad 26/60 Superdex column (2.6 × 60 cm). Protein concentrations were monitored by UV ($A_{1\ \mathrm{mg/mL}}^{280\ \mathrm{nm}} = 0.24$),[25] and YopH W354F yield was 120 mg.

Crystallization. All crystals were grown by hanging drop vapor diffusion at room temperature. Single crystals appeared 2 days after mixing 2 μL of protein solution (20 mg/mL in buffer A) and 3 μL of precipitant solution (12−19% polyethylene glycol 3350 and 0.1 M Hepes, pH 7.5). Optimization was subsequently achieved by microseeding. The apo W354F YopH crystals were grown in similar conditions using 0.1 M Tris buffer, pH 7.5. This step was required to eliminate extraneous electron density (presumably Hepes buffer) from the YopH active site. Indeed, sulfonates can competitively bind in the active site of PTPs;[8,29,30] e.g., YopH is inhibited by MES with a high K_i of 26 mM at pH 5.5.[8] Cryoprotection was performed by transferring crystals stepwise into stabilization solution with increasing glycerol amounts to a final concentration of 20%. The crystals then were flash-cooled in liquid nitrogen.

Crystals of YopH in complex with inhibitors were obtained by co-crystallization in solutions containing 5 mM Na_2WO_4 or Na_3VO_4; i.e., 0.5 μL of inhibitor solution (55 mM) was added to each drop. The orthovanadate solution was prepared by heating a stoichiometric amount of sodium metavanadate ($NaVO_3$) in 0.01 M NaOH, and the concentration was confirmed by UV at 260 nm.[31]

Data Collection, Structure Determination, and Refinement. Diffraction data were collected at the National Synchrotron Light Source (NSLS) at Brookhaven National Laboratory for the divanadate-bound structure and on a home source (Rigaku Raxis IV++) for the apo and tungstate-bound W354F YopH structures. Data for the apo and tungstate structures were indexed and processed using d*TREK in the program Crystal Clear,[32] and the divanadate structural data were handled using DENZO and SCALEPACK in the HKL2000 program suite.[33]

Table 1. Data Collection and Refinements for W354F YopH Apo and Co-crystallized Oxyanion-Bound Forms[a]

	apo	WO_4	V_2O_7
	Data collection		
beamline	home source	home source	NSLS X29
wavelength (Å)	1.5418	1.5418	1.0809
resolution range (Å)	29.8−1.65	26.4−1.69	29.1−1.42
outer shell (Å)	1.71−1.65	1.75−1.69	1.47−1.42
no. of reflections			
unique	35,018	31,969	54,027
total	147,195	252,942	449,419
average redundancy	4.2 (3.2)	7.9 (7.5)	8.3 (4.9)
mean $I/\sigma(I)$	25.8 (3.9)	39.4 (12.8)	30.8 (5.0)
completeness (%)	99.6 (99.0)	96.9 (93.2)	98.8 (89.5)
R_{merge} (%)[b]	2.7 (23.3)	3.5 (10.1)	6.5 (27.1)
space group	$P2_12_12_1$	$P2_12_12_1$	$P2_12_12_1$
unit cell dimensions (a, b, c (Å); $\alpha = \beta = \gamma = 90°$)	54.1, 58.4, 90.3	54.4, 58.3, 90.6	54.2, 58.3, 90.4
	Refinement		
R_{work}/R_{free} (%)[c]	19.8/23.4	17.5/20.7	17.4/19.6
atoms in the structure			
protein	2163	2163	2163
waters	268	373	310
ligands/ions	8	10	26
average B factors (Å^2)			
protein	22.31	13.44	18.54
water	34.00	28.54	33.14
ligands/ions	45.37	33.24	54.78
rmsd bond (Å)/angle (°)	0.012/1.4	0.011/1.2	0.008/1.4
protein geometry[d]			
Ramachandran outliers (%)	0.0	0.0	0.0
Ramachandran favored (%)	98.2	97.9	97.2
rotamer outliers (%)	0.4	0.8	0.8
PDB ID	3F99	3F9A	3F9B

[a] Values in parentheses correspond to the outer resolution shell. [b] $R_{merge} = (\sum|(I - \langle I\rangle)|)/(\sum I)$ where $\langle I\rangle$ is the average intensity of multiple measurements. [c] R factor was calculated using all data, $R_{factor} = (\sum|F_{obs} - F_{calc}|)/(\sum|F_{obs}|)$, and R_{free} is the same as R factor for a random 5% of reflections excluded from refinement. [d] The Ramachandran plot was calculated using the MolProbity server.[39]

Molecular replacement was performed using Phaser[34] from the CCP4 program suite,[35,36] with wildtype YopH (PDB ID 1YPT)[16] as a search model. Refinement was performed using Refmac5[37] from the CCP4 program suite. Coot[38] and MolProbity[39] were used for model building and validation. The crystallographic data and statistics of structure refinement are given in Table 1. The program PyMol[20] was used to prepare figures and superimpose structures. Structure factors and coordinates for the apo, tungstate, and divanadate structures have been deposited in the Protein Data Bank under accession numbers 3F99, 3F9A, and 3F9B, respectively.

Results

The crystallization of W354F YopH was carried out in the absence (apo enzyme) and in the presence of the oxyanions tungstate and vanadate. These ions are well-known inhibitors of PTPs, exhibiting strong affinity with $K_i < 100$ μM.[9]

(29) Wang, S.; Tabernero, L.; Zhang, M.; Harms, E.; Van Etten, R. L.; Stauffacher, C. V. *Biochemistry* **2000**, *39*, 1903–1914.
(30) Yuvaniyama, J.; Denu, J. M.; Dixon, J. E.; Saper, M. A. *Science* **1996**, *272*, 1328–1331.
(31) Gordon, J. A. *Methods Enzymol.* **1991**, *201*, 477–482.
(32) *CrystalClear*, 1.3.6 SP3 r6; Rigaku/MSC: Orem, UT, 2006.
(33) Otwinowski, Z.; Minor, W. *Macromol. Cryst. Pt. A* **1997**, *276*, 307–326.
(34) Mccoy, A. J.; Grosse-Kunstleve, R. W.; Adams, P. D.; Winn, M. D.; Storoni, L. C.; Read, R. J. *J. Appl. Crystallogr.* **2007**, *40*, 658–674.
(35) Bailey, S. *Acta Crystallogr., Sect D* **1994**, *50*, 760–763.
(36) Potterton, E.; Briggs, P.; Turkenburg, M.; Dodson, E. *Acta Crystallogr., Sect. D* **2003**, *59*, 1131–1137.
(37) Murshudov, G. N.; Vagin, A. A.; Dodson, E. J. *Acta Crystallogr., Sect. D* **1997**, *53*, 240–255.
(38) Emsley, P.; Cowtan, K. *Acta Crystallogr., Sect. D* **2004**, *60*, 2126–2132.
(39) Davis, I. W.; Leaver-Fay, A.; Chen, V. B.; Block, J. N.; Kapral, G. J.; Wang, X.; Murray, L. W.; Arendall, W. B., III; Snoeyink, J.; Richardson, J. S.; Richardson, D. C. *Nucleic Acids Res.* **2007**, *35*, W375–383.

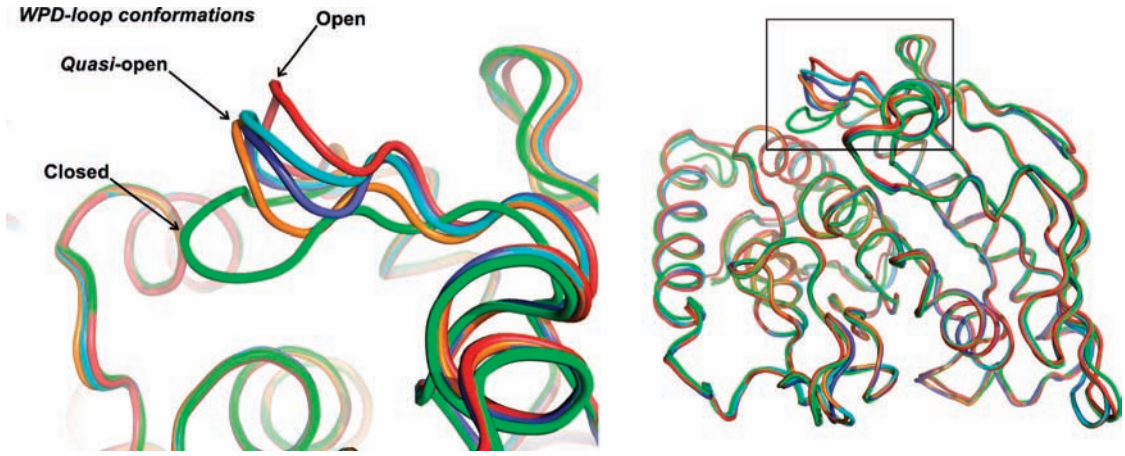

Figure 2. Comparison of native and W354F YopH structures. Superpositions compare the WPD conformations. Open WPD-loop: apo native YopH (1YPT,[16] red). Quasi-open WPD-loop: structures of YopH W354F apo form (in cyan) and in complex with divanadate (blue) and tungstate (orange). Closed WPD-loop: structure of native YopH in complex with tungstate (1YTW,[17] green). The image on the left is a magnification of the inset outlined on the right.

Conformation of the WPD-Loop. Structural superpositions of the YopH wildtype and W354F in apo and oxyanion-bound forms show that the W354F mutation has a significant effect on the conformation of the WPD-loop. The native YopH crystallizes with the WPD-loop in the open position, while oxyanion-bound structures show this loop in the closed position. As shown in Figure 2, in both the apo and oxyanion-bound forms of the W354F mutant, the WPD-loop adopts a conformation that is intermediate between the open and closed states of the native enzyme. We describe this newly observed conformation as a quasi-open conformation.

The WPD-loop is a dynamic region of YopH and other PTPs.[22,24,40] The distribution of *B*-factors along the protein sequence of YopH has been used previously to indicate changes in protein conformation.[19,24] Schubert et al. observed that the binding of sulfate to the active site of C403S YopH leads to decreased *B*-factors for the WPD-loop, suggesting that loop movement is restricted by complex formation.[19] In contrast, the *B*-factors in the WPD-loop of both the apo and bound forms of the W354F mutant increase by up to ~1.4 times when compared to the rest of the protein, indicating increased motion in this region.

In the apo wildtype structure, which contains two molecules in the asymmetric unit, the crystal contacts differ along the WPD-loop region, but the conformation of the loop is identical. In each case, the side chain of Thr358 forms a single hydrogen bond with a neighboring molecule. Similar interactions are not observed in the W354F structures which adopt the quasi-open conformation. It is possible that the fully open conformation is partially due to the Thr358 crystal contact; however, the structure approximates the fully open state suggested by MD simulations.[24] In the WPD-loop of the W354F mutant, the only residue involved in a crystal contact is the distal Ala 359, in which the carbonyl oxygen atom is hydrogen-bonded to the amide proton of Gly340 in an adjacent molecule. This single interaction is unlikely to affect the WPD-loop conformation. A figure representing this comparison can be found in the Supporting Information.

The quasi-open conformation has important consequences for the position of the general acid Asp356. In wildtype YopH, oxyanion binding and full WPD-loop closure involve a ~6 Å repositioning that brings the Asp356 into position for catalysis. In the W354F mutant, with or without a bound oxyanion, Asp356 occupies a position intermediate between the native open and closed states (Figure 3).

In the apo form, the conformation of the Arg409 side chain resembles that of the apo native YopH, and oxyanion binding causes similar conformational changes to this residue in the native enzyme and mutant. These changes include a 100° side chain rotation around χ^3 and formation of hydrogen bonds with the ligand's oxygen atoms. Further discussion of the relative positions of other, noncatalytic residues in the native and mutant structures, and other structural comparisons, can be found in the Supporting Information. The results presented here are focused on structural differences directly related to catalytic residues.

The position of Phe354 in W354F YopH closely matches that of Trp354 in the open state of the wildtype enzyme (Figure 4A). As found with Trp in native YopH, the Phe354 side chain slides into a hydrophobic crevice with restricted movement (Figure 4B), with van der Waals interactions on one side with the Arg409 side chain and Leu285, and on the other side with Val351, Val360, and Leu368. Structural comparisons between the open and closed WPD-loop conformations of wildtype YopH show that Trp354 rotates about 56° around the χ^2 dihedral angle as it moves from an open (71°; PDB ID 1YPT) to a closed (15°; 1YTW) conformation. In each of the W354F YopH structures, Phe354 remains in the same position, with the χ^2 dihedral angles ranging from 46 to 74° (~66° in apo form).

Modeling a Phe in the position of the five-membered ring of the indole moiety of W354 in the fully closed conformation of native YopH (Figure 5) produces significant steric clashes between the hydrogen atoms of the phenyl ring and the backbone of Pro355 and the side chain of Thr358 (Figure 5B) and other residues.

Oxyanion and Nucleophile Coordination Environments. Composite omit maps of the oxyanion binding site indicate strong agreement between the electron density and the tungstate and divanadate structures (Figure 6). For the divanadate structure,

(40) Peters, G. H.; Frimurer, T. M.; Andersen, J. N.; Olsen, O. H. *Biophys. J.* **2000**, *78*, 2191–200.

(41) Word, J. M.; Lovell, S. C.; Richardson, J. S.; Richardson, D. C. *J. Mol. Biol.* **1999**, *285*, 1735–1747.

(42) Word, J. M.; Lovell, S. C.; LaBean, T. H.; Taylor, H. C.; Zalis, M. E.; Presley, B. K.; Richardson, J. S.; Richardson, D. C. *J. Mol. Biol.* **1999**, *285*, 1711–1733.

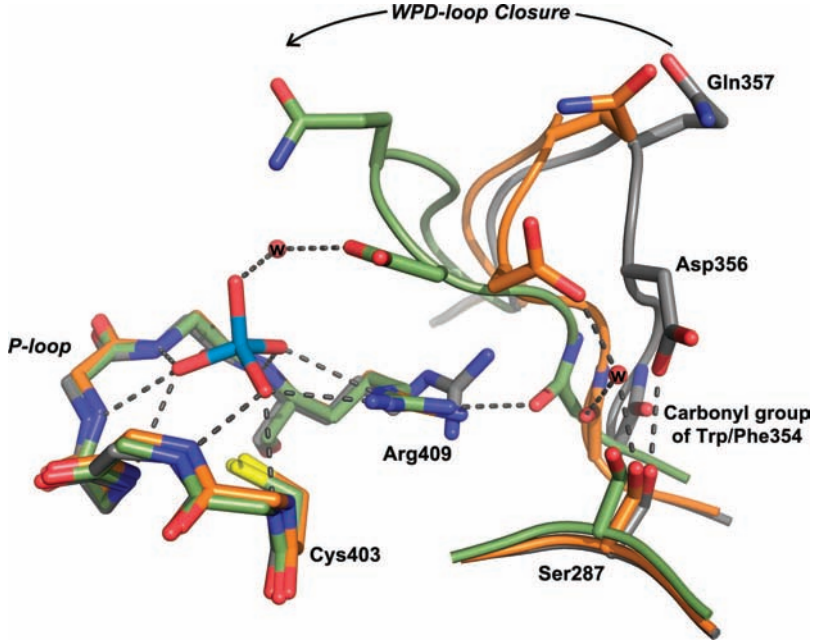

Figure 3. Comparison of W354F YopH in complex with tungstate (orange) with the native YopH apo (gray)[16] and tungstate (green)[17] structures, the latter two showing open and closed WPD-loop forms, respectively. The active site is formed by residues 403−409 in the P-loop and 354−362 in the WPD-loop. The bridging water molecules (balls with letter "w"), the tungstate anions, and the side chains of residues Asp356, Trp/Phe354, Cys403, and Arg409 are also shown. Hydrogen bonds are shown by dashed lines where distances between acceptor−donor atoms are shorter than 3.2 Å.

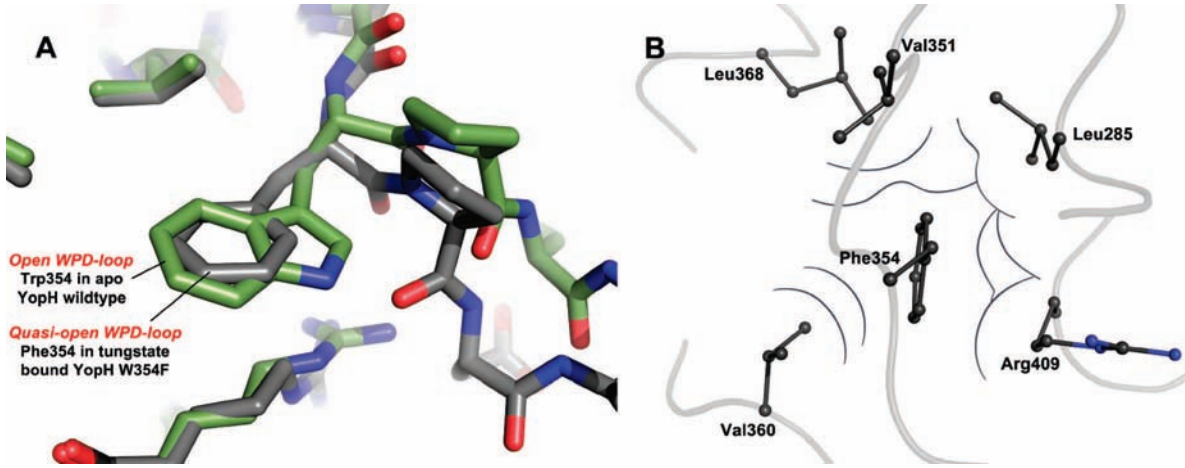

Figure 4. (A) Phe354 in the YopH mutant occupies a position similar to that of Trp354 in the wildtype enzyme. Atoms are colored according to type: carbons are gray (mutant) and green (wildtype), oxygens are red, and nitrogens are blue. (B) Phe354 resides in a hydrophobic crevice with restricted movement. The gray contour lines indicate regions of surface contact with Phe354. The structure in B is rotated ∼90° at the *y*-axis relative to the structure in A.

the electron density is essentially equivalent around each of the vanadium atoms, and the *B*-factors of the refined vanadium atoms are comparable to those of the atoms in the surrounding region, indicating that both sites are equally occupied. In other words, these data do not support the presence of a single vanadate molecule partially occupying the oxyanion binding site in two positions.

The oxyanions tungstate and divanadate bind in the P-loop of W354F YopH by an extensive hydrogen bond network involving the amide protons in the backbone of residues 404−409 and the Arg409 side chain (Figure 6).

At least eight hydrogen bonds are observed between the oxygen atoms of tungstate and P-loop residues in the W354F mutant, two of which involve Arg409 that rotates to interact with the oxyanion. These interactions favor closure of the WPD-loop in the YopH wildtype[17] and C403S mutant[19] but, in contrast, do not significantly affect the WPD-loop conformation in the W354F mutant.

The negative sulfur atom of Cys403 resides at the bottom of the active-site pocket and is oriented toward the electrophilic tungsten atom of the WO_4^{2-} ion. Tungsten−sulfur distances of about 3.2 Å in the W354F mutant structures are close to those observed in wildtype YopH with tungstate bound (∼3.5 Å). The anionic sulfur of Cys403 is stabilized as observed in the YopH wildtype structure.[16] The thiolate is immersed in a positive electrostatic environment with hydrogen bonds to backbone amide groups of Gly406 at 3.4 Å and Thr410 at 3.6 Å, in addition to the hydroxyl group of Thr410 at 3.2 Å.

The interactions between the oxyanion and Gln357 and Asp356 in the closed WPD-loop conformation in wildtype YopH are absent in the W354F mutant due to the quasi-open conformation of the WPD-loop. This is in agreement with the

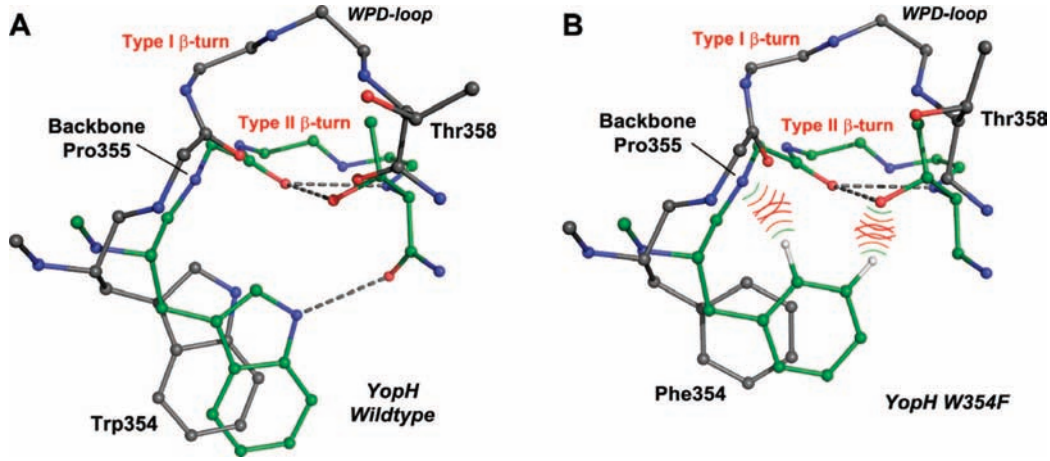

Figure 5. Conformational changes in the WPD-loop of YopH wildtype and W354F mutant. Upon closure, the WPD-loop changes from a type I (gray) to a type II β-turn (green). (A) In YopH wildtype, Trp354 slides ~1.6 Å orthogonally into the crevice, and the indole N−H hydrogen-bonds to the carbonyl oxygen of Thr358. Structures were drawn from apo and tungstate-bound YopH, PDB ID 1YPT and 1YTW, respectively. (B) Similar representation considering the Phe mutant showing that complete WPD-loop closure would be accompanied by prohibitive clashes (in curved lines) with the backbone of Pro355 and the hydroxyl group of Thr358. The structure in gray is the apo form of YopH W354F. The clashes were generated from the hypothetical structure in green. The model was built from the structure of the wildtype YopH in complex with tungstate (PDB ID 1YTW) by replacing the tryptophan with a phenylalanine. Model building was performed using Coot, hydrogen atoms were added with Reduce,[41] and clashes and contacts were generated by Probe.[42]

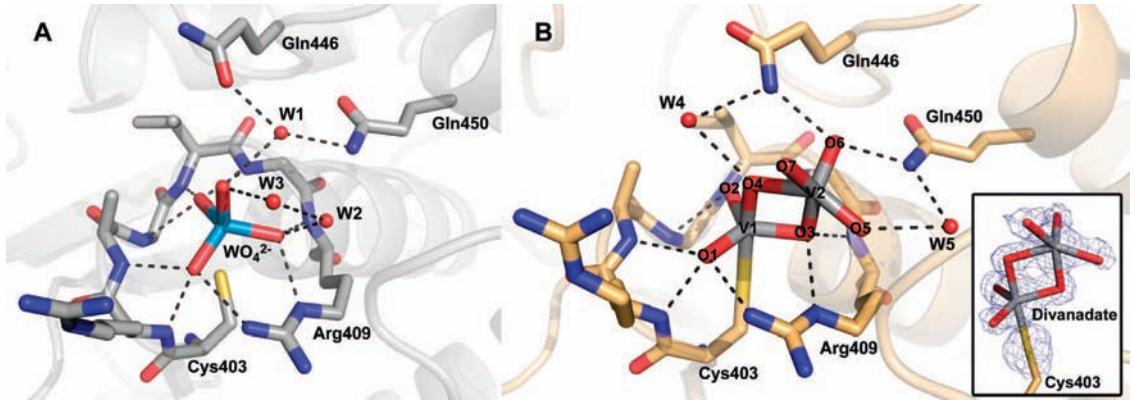

Figure 6. Binding environment for tungstate (A) and divanadate (B) in the active site of W354F YopH. Hydrogen bonds are shown by dashed lines, and the acceptor−donor atom distances are shorter than 3.2 Å. Inset: Composite omit electron density map for divanadate generated at 1.5σ contour level.

higher oxyanion inhibition constants observed for catalysis by the W354F mutant. For example, tungstate inhibits wildtype YopH with $K_i = 5.8$ μM at pH 5.5, while $K_i = 32$ μM with the W354F mutant.[9]

Divanadate Moiety. The interaction between monomeric vanadate and PTPs is typically strong and is promoted by the nucleophilic attack of the cysteine sulfur atom on the vanadium atom. This interaction yields a trigonal bipyramid structure that differs from the divanadate structure in the active site of W354F YopH, which exhibits a double distorted trigonal bipyramid containing a cyclic $[VO]_2$ core (Figure 6). The axial bond lengths V1−S and V1−O_4 are 2.5 and 2.1 Å, respectively, similar to axial bonds previously observed in PTP structures with monomeric vanadate.[43−45] In other PTP structures the V1−$O_{equatorial}$ bonds are ~0.2 Å longer than V1−O_{axial}. In the W354F YopH structure, one V1−$O_{equatorial}$ bond exhibits the same length seen in monomeric structures, while the others are shorter by ~0.1 Å. The V2 atom is coordinated into a distorted trigonal bipyramid, in which the bridging oxygens O4 and O3 are 2.1 Å from V2, respectively, while the other three V2−oxygen distances are 1.9 Å. The O6 atom hydrogen-bonds to the N−H atoms of glutamines 446 and 450, the O5 atom to a water molecule, and O7 to the amino group of Lys447.

Active-Site Waters. Several water molecules are found at the active site (designated by "w" in Figure 6). Their *B*-factors, which are measures of structural mobility,[46] generally agree with those of surrounding protein residues and indicate that these waters are well-ordered. In the structure of the apo W354F mutant, three water molecules adopt positions similar to those observed at the active site of other PTPs, such as PTP1B, SHP-2, PTPμ, and PTP LAR.[47] Oxyanion binding displaces all three water molecules, in agreement with observations in other PTP−inhibitor complexes. In the apo structure, these water molecules assume virtually the same positions occupied by the

(43) Denu, J. M.; Lohse, D. L.; Vijayalakshmi, J.; Saper, M. A.; Dixon, J. E. *Proc. Natl. Acad. Sci. U.S.A.* **1996**, *93*, 2493–2498.
(44) Pedersen, A. K.; Guo, X. L.; Moller, K. B.; Peters, G. H.; Andersen, H. S.; Kastrup, J. S.; Mortensen, S. B.; Iversen, L. F.; Zhang, Z. Y.; Moller, N. P. H. *Biochem. J.* **2004**, *378*, 421–433.
(45) Evdokimov, A. G.; Pokross, M.; Walter, R.; Mekel, M.; Cox, B.; Li, C. Y.; Bechard, R.; Genbauffe, F.; Andrews, R.; Diven, C.; Howard, B.; Rastogi, V.; Gray, J.; Maier, M.; Peters, K. G. *Acta Crystallogr., Sect. D* **2006**, *62*, 1435–1445.
(46) Yuan, Z.; Bailey, T. L.; Teasdale, R. D. *Proteins* **2005**, *58*, 905–912.
(47) Pedersen, A. K.; Peters, G. H.; Moller, K. B.; Iversen, L. F.; Kastrup, J. S. *Acta Crystallogr., Sect. D* **2004**, *60*, 1527–1534.

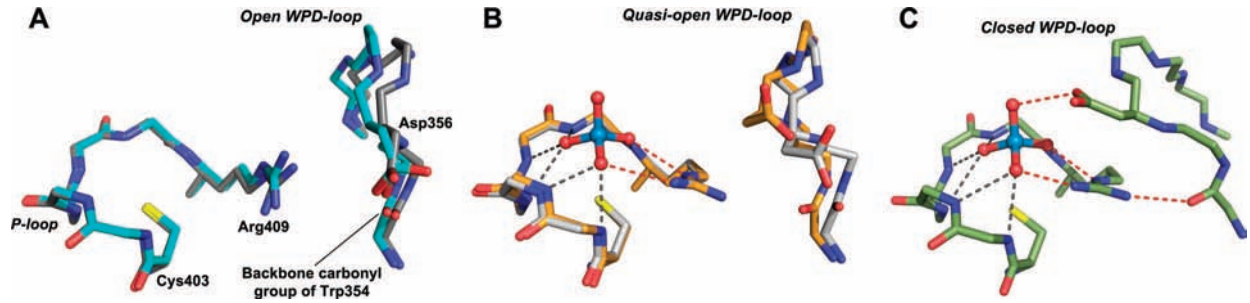

Figure 7. Snapshots from X-ray crystallography structures showing events on the pathway between substrate/oxyanion binding and complete closure of the WPD-loop. (A) Open WPD-loop, apo forms of the native (dark gray) and W354F mutant YopH (light blue). (B) Quasi-open conformation, tungstate- (orange) and divanadate- (gray) bound forms of W354 mutant (only tungstate is shown). (C) Closed WPD-loop, tungstate-bound form of the native YopH (green). Hydrogen bonds are shown by dashed lines for distances between acceptor−donor atoms shorter than 3.2 Å. Dashed lines in gray are those between the oxyanion and the P-loop backbone.

three oxygen atoms of WO_4^{2-} that hydrogen-bond to the P-loop in the tungstate structure. In the structure with tungstate, water molecule W1 is coordinated by the nitrogen atoms of glutamines 446 and 450 (Figure 6A). In the structure with divanadate, several oxygen atoms of the ligand occupy the positions of water molecules co-crystallized with tungstate. These water molecules include W1 that is replaced by the O6 atom, and W2 and W3 that are replaced by O5 and O7, respectively (Figure 6).

The waters observed at the active site of apo W354F are relevant to the energy penalty associated with displacement of water molecules from the active site during substrate binding. They can also contribute to inhibitor binding by acting as bridges in the formation of hydrogen bonds between inhibitor and enzyme and by dispersing charge.[47] This is demonstrated in a crystal structure of PTP1B (2AZR), in which binding of the competitive inhibitor 3-(carboxymethoxy)thieno[2,3-*b*]pyridine-2-carboxylate ($K_i = 200\ \mu$M at pH 5.5) is mediated by hydrogen bonds involving two of the P-loop water molecules, and results in WPD-loop closure.[48]

Discussion

The impaired position of the WPD-loop in W354F YopH provides a structural explanation for the significantly altered kinetics reported previously.[9,25] Mutation of Trp354 to phenylalanine was found to reduce the efficiency of general acid catalysis and resulted in a 10^2-fold reduction of k_{cat}. Kinetic isotope effects revealed that proton transfer to the substrate leaving group is only half complete in relation to the native enzymatic reaction, in which protonation is fully synchronized with P−O bond fission and the leaving group is uncharged in the transition state.[25] Mutation of Trp354 to Ala results in more drastic consequences, with general acid catalysis completely disabled and the leaving group bearing essentially a full negative charge in the transition state. The results obtained in this study give a structural explanation for these data and indicate that, during catalysis by the W354F mutant, the general acid assumes a position permitting only partial proton transfer in the transition state.

WPD-Loop Dynamics. Hu and Stebbins[24] reported MD simulations to probe the time scale of WPD-loop opening/closure. In calculations with the native apo YopH, the distance between the α-carbon atoms of Gln357 and Val407 fluctuates from 17 Å in the open to ∼13 Å in a partially closed conformation with a frequency of ∼4 ns. In contrast, the corresponding distance in the crystal structure of the closed conformation of native YopH in complex with a bound oxyanion is about 11 Å. As the authors indicated,[24] loop closure is not complete in their simulations because closure is probably induced by ligand binding and therefore may not occur, at least in the same form, in the apo enzyme. Here, we observe that the Gln357−Val407 distances in W354F YopH in complex with oxyanions range from 15 to 13 Å, which, according to Hu and Stebbins, are values expected for partial WPD-loop closure. We refer to this as a quasi-open WPD-loop conformation, in contrast to the closed forms in which the general acid (Asp356) is at the critical distance permitting full proton transfer to the leaving group during catalysis. The similarity between the WPD-loop positions in the unbound and oxyanion-bound W354F structures (Figure 2) indicates that impairment of the WPD-loop from the mutation exists both in the presence and in the absence of bound oxyanion.

Binding of the substrate and rotation of Arg409 create the conditions for an equilibrium favoring the closed conformation, which places Asp356 into position for general acid catalysis. Figure 7 summarizes the first steps as snapshots of WPD-loop movement to accomplish the closed conformation: (A) the WPD-loop is open and the arginine side chain is free. (B) Oxyanion binds in the P-loop and Arg409 rotates to make hydrogen bonds with the oxyanion. The WPD-loop is a dynamic region, and residues 357−363 move into the active site. The Asp356 residue rotates counterclockwise and swings into the active site. This rotation may occur through a bridge interaction involving a water molecule (see Figure 3), although we presume this to be less important when Asp356 is protonated. (C) The new conformation of Arg409 creates favorable conditions for interaction with the WPD-loop, including a hydrogen bond between the carbonyl oxygen of Trp354 and Arg409. This last step brings the WPD-loop to the closed and active conformation.

The quasi-open conformation of the WPD-loop in the W354F mutant can be rationalized by modeling a Phe in the position of the W354 in the fully closed conformation (Figure 5). Placing a Phe in the position of the five-membered ring of the indole moiety in the closed conformation produces significant steric clashes between the hydrogen atoms of the phenyl ring and the backbone of Pro355 and the side chain of Thr358 (Figure 5B). Additional changes in the Phe conformation cause clashes with other residues that flank Phe354 (see Figure 4B). These clashes presumably disrupt the secondary structure of the WPD-loop and appear to be resolved by retaining the catalytically inactive type I conformation. Furthermore, the Phe ring is unable to form

(48) Moretto, A. F.; Kirincich, S. J.; Xu, W. X.; Smith, M. J.; Wan, Z. K.; Wilson, D. P.; Follows, B. C.; Binnun, E.; Joseph-McCarthy, D.; Foreman, K.; Erbe, D. V.; Zhang, Y. L.; Tam, S. K.; Tam, S. Y.; Lee, J. *Bioorg. Med. Chem.* **2006**, *14*, 2162–77.

the hydrogen bond that is observed between W354 and the backbone carbonyl of Thr358 in the native enzyme (Figure 5A).

To date, small protein models showing general acid catalysis reveal that efficient catalysis occurs only when a critical distance between the general acid and the leaving group oxygen can be reached and kept for the time necessary to transfer.[26,27] Crystal structures of native YopH with bound oxyanions suggest that the proton of Asp 356 resides ~2 Å from the leaving group oxygen in the catalytically productive, closed conformation. The impaired general acid catalysis in the W354F mutant arises from the distance dependence of the general acid in relation to the leaving group oxygen. If the Asp356 in the W354F YopH structure with tungstate bound (Figure 3) is rotated toward the leaving group oxygen to optimize this distance, the oxygen proton donor and the leaving group oxygen are ~4.3 Å apart and probably cannot move much closer because of prohibitive clashes with the β-turn configuration of the WPD-loop. If this reflects the situation in solution, then general acid catalysis in W354F may only feasibly occur via a bridging water molecule between the carboxylic acid and the leaving group oxygen. Kinetic isotope effects (KIEs) demonstrate that inefficient general acid catalysis still occurs, with the leaving group about half-neutralized in the transition state. The possibility that this partial neutralization is provided by buffer, with the carboxylate of Asp 356 having no role, is argued against by the fact that KIEs with a general acid mutant at the same pH indicate a completely ionized leaving group.[49]

Catalysis by PTPs depends in part on proper positioning of the substrate to achieve high effective molarity of the nucleophilic cysteine and of the general acid catalyst. Studies with model systems indicate that proton transfer requires particularly precise positioning in order to optimize catalysis.[28] The structures indicate that the expanded donor−acceptor distance from 2 Å in native YopH to 4.3 Å in W354F accounts for the change from full leaving group neutralization in the transition state to about half-neutralization revealed by KIEs. The KIEs probe the first reaction, phosphoryl transfer from substrate to enzyme. The Asp functions as a base to deprotonate water in the subsequent hydrolysis of the phosphoenzyme, and the greater distance will presumably adversely affect that reaction as well.

Divanadate Moiety at the Active Site. Monomeric vanadium species are well-known inhibitors of phosphatases and have been observed in a number of crystal structures. The divanadate observed here is an unusual structure which, to our knowledge, has not been previously reported in protein crystallography. Reports of vanadate species in protein crystallography have been restricted to monomeric[45,50,51] and some polymeric species, including trivanadate[52] and decavanadate.[50] A solution ^{51}V NMR study has reported observation of a divanadate ion bound to each of the two active sites of rabbit muscle phosphoglycerate mutase.[53]

Table 2. Selected Structural Parameters of the Divanadate Anion (V_2O_7) Bound in W354F YopH and of a Related Dimeric Complex, $\{[VO_2(OC_2H_4S)]_2\}^{2-}$ (**2**),[57] Containing a Central $[VO]_2$ Core[a]

	V_2O_7	$\{[VO_2(OC_2H_4S)]_2\}^{2-}$
V1−S	2.5	2.38
V1−O1; V1−O2	1.9	1.62
V1−O3; V1−O4	2.0	2.00
V2−O3; V2−O4	2.1	2.00
O3−V1−O4	82	69.9
V1−O3−V2	97	110.1
V1−O3−V2-O4	1	0.0

[a] Interatomic distances are in angstroms, and angles are in degrees.

The solution chemistry of vanadium(V) is complex[54,55] and is briefly summarized in the Supporting Information. The predominant divanadate species in the pH range 7−7.5 is $H_2V_2O_7^{2-}$. In solution, it is believed that divanadate has the same structure and conformation observed in the solid state, which consists of two VO_4 tetrahedral moieties in vertex style **1**.[54]

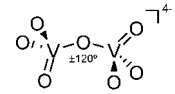

1

It is important to point out that there is no precedent in the literature for a divanadate species in solution exhibiting the cyclic $[VO]_2$ core observed at the active site of the W354F mutant. NMR spectra (results not shown) for the vanadate solution prepared from $NaVO_3$ as described in the Materials and Methods, as well as from a solution of Na_3VO_4, each exhibit the same speciation profile reported in the literature.[53,56] However, several small molecule X-ray structures provide precedent for divanadate in the geometry depicted in Figure 6.[55] Table 2 compares the structural parameters of the species reported here with those for the dimeric complex $\{[VO_2(OC_2H_4S)]_2\}^{2-}$ (**2**).[57] The cyclic $[VO]_2$ core structure both in the enzymatic structure and in $\{[VO_2(OC_2H_4S)]_2\}^{2-}$ share structural characteristics, exhibiting distorted trigonal bipyramidal arrangements around the cyclic $[VO]_2$ core.

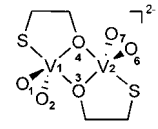

2

The divanadate species observed in the active site of W354F YopH may arise from the reaction depicted in Scheme 2.

The divanadate is a double tetrahedral vertex, and therefore nucleophilic attack of Cys403 leads to a bipyramid coordination. The bond between the vanadium and the axial oxygen is longer than the equatorial bonds, and the pK_a should be sufficiently high to guide a second nucleophilic attack of the axial oxygen on the second vanadium atom. Stabilization of this structure occurs by distortion of the double bipyramid system and coordination to the active site. In fact, it likely that the cyclic $[VO]_2$ core provides stability to the complex.[57] Since the native enzyme is bound with a single vanadate ion (PDB code 2I42),

(49) Hengge, A. C.; Sowa, G. A.; Wu, L.; Zhang, Z.-Y. *Biochemistry* **1995**, *34*, 13982–13987.
(50) Felts, R. L.; Reilly, T. J.; Tanner, J. J. *J. Biol. Chem.* **2006**, *281*, 30289–30298.
(51) Zhang, M.; Zhou, M.; VanEtten, R. L.; Stauffacher, C. V. *Biochemistry* **1997**, *36*, 15–23.
(52) Rigden, D. J.; Littlejohn, J. E.; Henderson, K.; Jedrzejas, M. J. *J. Mol. Biol.* **2003**, *325*, 411–420.
(53) Stankiewicz, P. J.; Gresser, M. J.; Tracey, A. S.; Hass, L. F. *Biochemistry* **1987**, *26*, 1264–1269.
(54) Cruywagen, J. J. *Adv. Inorg. Chem.* **2000**, *49*, 127–182.
(55) Crans, D. C.; Smee, J. J.; Gaidamauskas, E.; Yang, L. Q. *Chem. Rev.* **2004**, *104*, 849–902.
(56) Rehder, D. *Bull. Magn. Reson.* **1982**, *4*, 33–83.
(57) Bhattacharyya, S.; Batchelor, R. J.; Einstein, F. W. B.; Tracey, A. S. *Can. J. Chem.* **1999**, *77*, 2088–2094.

Scheme 2. Probable Pathway for Formation of the Divanadate Anion Containing a Cyclic $[VO]_2$ Core in the Active Site of W354F YopH[a]

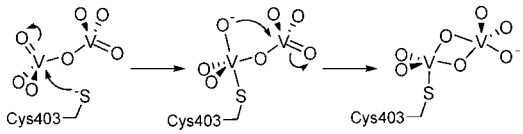

[a] Charges are shown only in positions involved in an apical attack to give a bipyramidal geometry as explained in the text. Charges are omitted from other oxygen atoms because of the uncertain protonation state.

the impaired position of the WPD-loop in the YopH mutant may be important in stabilizing the unusual divanadate anion.

Conclusion

Oxyanion binding in the P-loop of the W354F mutant shares some structural characteristics with the native enzyme. However, in the W354F mutant the WPD-loop is in a quasi-open conformation. This impaired conformation has not been observed in crystal structures but resembles one of the intermediate loop positions observed in molecular mechanics simulations of loop closure. The WPD-loop seems to be locked in an unfavorable position that permits the general acid carboxylate to come within about 4.3 Å of the leaving group oxygen atom, more than 2 Å farther than native YopH. The longer distance permits only partial neutralization of the leaving group in the transition state detected in previous studies. This has significant consequences for general acid catalysis that result in a reduction of 10^2-fold for k_{cat}.[25] It is likely that the less efficient acid catalysis most likely occurs via an intervening water molecule.

One can presume that small molecules that could similarly lock the WPD-loop could be used as a potentially alternative strategy to inhibit PTPs. Such a strategy might avoid the need for recognition by the P-loop and circumvent the necessity of highly polar inhibitors, since interaction and recognition involving the WPD-loop can occur at the surface and at the hydrophobic crevice of the active site.

The divanadate species observed at the active site is, to our knowledge, the first enzyme-bound polyvalent vanadate exhibiting a bipyramid trigonal conformation. This complex has a cyclic $[VO]_2$ core, and its formation seems to be catalyzed by the attack of the nucleophilic cysteine. This species is stabilized by additional interactions at the top of the active site. These findings are important for further studies. Vanadate is a structural transition state analogue for phosphoryl transfer, and it is commonly used in crystallographic and kinetic studies with PTPs. *In vivo* and *in vitro* studies have demonstrated biological effects of vanadium ions. Monovalent vanadate has been proposed as a potential PTP inhibitor with insulin-mimetic effects in humans,[58] while the polyvalent decavanadate has exhibited noradrenaline-mimetic activities.[59] Although intracellular concentrations of vanadium are too low to favor the formation of polymeric species, these have inherent stability. Therefore, under therapeutic doses, polyvanadate species may accumulate *in vivo*.[59]

Acknowledgment. We thank Dr. Z.-Y. Zhang for providing the plasmid encoding the W354F YopH, and Dr. Debbie Crans for helpful discussions about vanadium chemistry. We are also grateful to CAPES (Brazil) for a Fellowship to T.A.S.B. This research was supported by a grant from the National Institutes of Health (GM47297) to A.C.H. Financial support for use of the NSLS comes principally from the Offices of Biological and Environmental Research and of Basic Energy Sciences of the U.S. Department of Energy, and from the National Center for Research Resources of the National Institutes of Health.

Supporting Information Available: Figure showing the crystal contacts at the vicinity of the WPD-loop, additional discussion of structural comparisons between the W354F mutant and native YopH, and summary of vanadate speciation in solution. This material is available free of charge via the Internet at http://pubs.acs.org.

JA807418B

(58) Thompson, K. H.; Orvig, C. *J. Inorg. Biochem.* **2006**, *100*, 1925–1935.
(59) Aureliano, M.; Gandara, R. M. *J. Inorg. Biochem.* **2005**, *99*, 979–985.